Journal of Ocean, Mechanical and Aerospace
-Science and Engineering-, Vol.23

September 20, 2015

Prediction of Non-Cavitating Marine Propeller Noise

K.L.Satyavarma, [a,*] and C. Neelima Devi, [b]

[a)] *Department of Mechanical Engineering, University College of Engineering Vizianagaram, JNTUK, INDIA*
[b)] *Department of Mechanical Engineering, University College of Engineering Vizianagaram, JNTUK, INDIA*

*Corresponding author: satyavarma43@gmail.com

Paper History

Received: 7-August-2015
Received in revised form: 11-September-2015
Accepted: 20-September-2015

ABSTRACT

Noise reduction and control is an important problem in the performance of underwater acoustic systems. As the propeller rotates, it is subjected to unsteady force, which leads to discrete tonal noise, and cavitation. Therefore, underwater propeller noise can be classified into cavitating and non-cavitating noise Furthermore, sound generated by a propeller is critical in underwater detection and it is often related to the survivability of the vessel. This paper presents a numerical study on noises of the underwater propeller for different performance conditions. The non-Cavitating noise generated by an underwater propeller is analyzed numerically in this study. The flow field is analyzed with finite volume method (FVM), and then the acoustic analysis is made by the use of Ffowcs Williams–Hawkings (FW-H) formulation to predict the far-field acoustics at different operating conditions. Noise characteristics are presented according to different positions of hydrophones and speeds of the propeller. Computed results are shown to be in good agreement with experimental results.

KEY WORDS: *Propeller Noise; FVM; FW-H; Hydrophone.*

NOMENCLATURE

δ (f)	Dirac delta function,
H (f)	Heaviside function,
T_{ij}	Light hill stress tensor,
P_{ij}	Compressive stress tensor,
P’	Sound pressure at the far-filed

1.0 INTRODUCTION

Unwanted sound of vibration is called as noise. The four principal groups of radiated noise sources are (a)Machinery vibration caused by propulsion (b)machinery and ships’ services and (c)auxiliary machinery, including steam, water, and (d)hydraulic piping systems. In this paper we considered only non-cavitating marine propeller induced noise. Münir Cansın Özden1 [1] the objective of the present work is to conduct a numerical prediction of the acoustic field generated by a marine propeller in non-uniform inflow. To consider the effect of the interaction between the unsteady propeller loading and incoming non-uniformities, we use the DES method to account for the nonlinear viscous flow field over the rotating blades. The far-field radiation is calculated by a retarded-time integral formula solving the FW-H (Ffowcs Williams-Hawkings) equation, with the solution of the DES taken as the input data. The hydrodynamic and Hydroacoustic performances of DTMB4118 propeller encountering with inflows of two different cyclic distortions are compared and discussed. Bagheri M.R [2] this work is carried out using CD-Adapco's StarCCM+ CFD package, which has a built-in acoustic model, in the form of the Ffowcs-Williams Hawkings (FW-H) equation. The Ffowcs-Williams Hawkings equation uses generalized functions to extend the application of Lighthill's Acoustic Analogy, which is originally used to predict the aerodynamic noise generated by rotating bodies such as helicopter rotors and fan blades. More recently this equation has also been applied to operations in other fluids, namely water, for the noise generated by marine propellers. In situations where detailed data on the turbulent phenomena in the near-field can be obtained, the Ffowcs-Williams Hawkings equation can also be used for broadband noise prediction. Morgut, M [3] this paper presents a numerical study on noises of the underwater propeller for different performance conditions. The non-cavitating and blade sheet cavitation noise generated by an underwater propeller is analyzed numerically in this study. The noise is predicted using time-domain acoustic analogy. [6] The objective of the current study is to analyze resistance and self-propulsion characteristics

of MS791 depending on different skew geometries and to obtain useful information for further investigation of twin-skew ships with podded Propulsors. [7] Viscous Computational Fluid Dynamics (CFD) simulations for towed and self-propelled conditions of MS791 are performed using Reynolds Averaged Navier-Stokes (RANS) solver SURF ver.6.44 (Hino 1997) developed by CFD research group in NMRI. [4]Hand book of Acoustics by Malcolin J.Crocker, in different types of noises and their effects and the propeller characteristics were explained. [5] The effects of noises in the marine propellers and their effects and remedies are explained in the book of Marine Propellers and Propulsions by John Carlton.

2.0 THEORETICAL BACKGROUND

2.1 Propeller Non-Cavitating Noise

There are three types of non-cavitating noise:

- Mechanical blade tonal related to propeller shaft speed and the number of blades.
- • Propeller broadband noise related to blade vibratory response to turbulence in gestation and trailing edge vortices.
- Propeller singing due to coincidence of vortex shedding and blade resonant frequencies.

Blade tonal and harmonics result from oscillating components of forces or propeller thrust variations caused by circumferential variations of the wake inflow velocity.

2.2 Factors to Be Considered To Control Noise

Significant reductions in propeller noise have been achieved through smoothing and control of inlet flows and the design of skewed blades. The flow speed varies from 10-90% of the forward speed of the propeller. These velocity differences cause large variations of the angle of attack and associated lift forces, which lead to significant fluctuations in thrust and torque during each revolution of the shaft and in turn to high level, low frequency hull vibration. Thus, the most important design consideration is the relationship between the harmonic structure of the wake and the number and blade form of the propellers. The primary propeller design factors include diameter, shaft rpm, and number of blades, expanded area ratio, load distribution, skew distribution, blade tip hull clearance, and the spatial and temporal characteristics of the inflow field

In the present case propeller consists of five blades. The diameter of propeller is 0.4 m and hub to propeller diameter is 0.389. In the present simulations for prediction of non-cavitating noise of propeller is carried out at rotating speed of propeller at 780rpm & 840rpm and the flow speed at 6.66m/s & 7.17m/s. The noise produced by a propeller is very much importance to warship designers and military strategists for many years. So in this case an attempt is made to prediction of non-cavitation noise of propeller using of FW-H equation coupled with DES computer code based on cell-centered finite volume method (FVM) on unstructured meshes for viscous flow field around propeller. These results are compared with experiments conducted in cavitation tunnel of size 1x1x6m.

Noise radiated directly by propeller blades includes discrete frequency lines (tonal) in the low to mid frequency range and broadband noise with a continuous spectrum. The FW-H method has been adopted here for prediction of discrete frequency spectra resulting from fluid-structure interaction at the trailing edge of the propeller blades. In particular, the formulation is provides a solution for the monopole and dipole tonal sources for a given geometry, displacement and aerodynamic loading of the moving bodies. The implementation of this formulation is quite straight forward because the contributions from each propeller surfaces with different retarded times can be added to form an acoustic wave. The solutions need an estimation for the retarded times and an accurate representation for the blade loading.

2.3 Flow Solver

DES (Detached-Eddy Simulation)

The difficulties associated with the use of the standard LES models, particularly in near-wall regions, has led to the development of hybrid models that attempt to combine the best aspects of RANS and LES methodologies in a single solution strategy. An example of a hybrid technique is detached-eddy simulation (DES) [8] Spalart et al (1997) approach. This model attempts to treat near-wall regions in a RANS-like manner, and treat the rest of the flow in an LES-like manner. The model was originally formulated by replacing the distance function d in the Spalart-Allmaras (S-A) model with a modified distance function d'= min [d, CDES Δ], where CDES is a constant and Δ is the largest dimension of the grid cell in question. This modification of the S-A model, while very simple in nature, changes the interpretation of the model substantially. This modified distance function causes the model to behave as a RANS model in regions close to walls, and in a Smagorinsky-like manner away from the walls. Rui Z., Chao Y [10]DES does not require the grid resolution in the near wall region as fine as LES would while it still works like LES in the region away from the wall where the large scale structures are formed and convicted. Sliding mesh technique was employed to deal with the rotary motion

2.4 Ffowcs Williams Hawkings Equation

As discussed earlier, simulation has been carried out with the FW-H formulation. The FW-H equation is an inhomogeneous wave equation that is derived by manipulating the continuity equation and the Navier-Stokes equations. It is given by

$$\frac{1}{a_0^2}\frac{\partial^2 p'}{\partial t^2} - \nabla^2 p' = \frac{\partial^2}{\partial x_i \partial x_i}\{T_u H(f)\} - \frac{\partial}{\partial x_i}\{[P_u n_i + \rho u_2(u_n - v_n)]\delta(f)\} + \frac{\partial}{\partial t}\{[\rho_0 v_n + \rho(u_n - v_n)]\delta(f)\} \quad (1)$$

Here ui is fluid velocity component in the xi direction, un is fluid velocity component normal to the surface f=0, vi is surface velocity component in the xi direction, Vn is surface velocity component normal to the surface, δ (f) is Dirac delta function, H (f) is Heaviside function, Tij is Lighthill stress tensor, Pij is compressive stress tensor, P' is sound pressure at the far-filed (p' = p – p0). The solution to above Equation is obtained using the free-space Green's function.

The complete solution consists of surface integrals and volume integrals. The surface integrals represent the contributions from monopole and dipole acoustic sources and partially from quadrupole sources, whereas the volume integrals represent

quadrupole (volume) sources in the region outside the source surface. The contribution of the volume integrals becomes small if Mach number is low and the source surface is enclosed. Therefore Fluent offers surface integral solution only, which is applicable for marine propeller.

3.0 NUMERICAL SIMULATION

In this paper, one type propeller model of NACA series was used for investigations. The majority of the users used variants of 'projection methods' or what may be called 'pressure-based methods' such as SIMPLE and PISO to satisfy the continuity equation and to advance the solution in time. The flow solution procedure is the SIMPLE routine. To simulate the cavitating flow the numerical code FLUENT was used. The code uses a control-volume-based technique to convert the governing equations in algebraic equations that can be solved numerically. This control volume technique consists of integrating the governing equations at each control volume, yielding discrete equations that conserve each quantity on a control-volume basis. This solution method is designed for incompressible flows, thus being implicit. The full Navier-Stokes equations are solved. The flow was assumed to be steady, and isothermal. In these calculations turbulence effects were considered using turbulence models, as the DES models, with the modification of the turbulent viscosity for multiphase flow [9] Sebastien D. To model the flow close to the wall, the standard wall-function approach was used, and then the enhanced wall-function approach has been used to model the near-wall region (i.e., laminar sub layer, buffer region, and fully-turbulent outer region). For this model, the used numerical scheme of the flow equations was the segregated implicit solver. For the model discretization, the SIMPLE scheme was employed for pressure-velocity coupling, second-order upwind for the momentum equations, and first-order upwind for other transport equations (e.g., vapor transport and turbulence modeling equations).

3.1 Computational Mesh

Modeling, geometry, computational domains, boundary conditions, topology, meshing method and mesh size and turbulent method have significant effects on a fruitful numerical analysis and accuracy of simulation. Meshing strategy is divided in two divisions. Hybrid unstructured a mesh means that the tetrahedral elements for flow fluid fields, while structured mesh means that the hexahedral mesh is totally used for meshing on the solid surfaces. In contrast, the results of simulations with structured mesh elements usually have more accuracy than tetrahedral mesh elements results.

Unstructured mesh elements production is almost automatic while hexahedral mesh elements generation is not automatic and should be generated manually. On the other hand, for flow field meshing, sometimes, the geometry is not compatible to use the hexahedral mesh elements, so unstructured mesh elements have better results and convergence of solution is nice. Therefore, we used the hybrid unstructured mesh elements for domain, in which we utilized the stationary and rotational domain for full scale propeller simulation with five blades. Auto mesh option is used in this project.

The flow domain is required to be discretized to convert the partial differential equations into series of algebraic equations. This process is called grid generation. The meshed figure of the propeller enclosed with its domain is shown below:

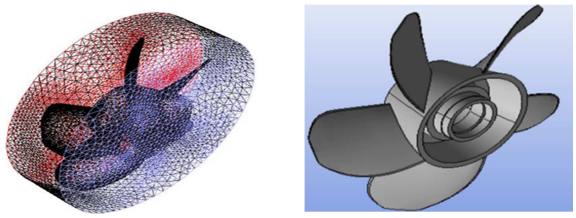

Figure 1: Geometry & meshed model of the propeller with its domain.

The inlet was considered at a distance of 0.15D (where D is diameter of the propeller) from mid of the chord of the root section. Outlet is considered at a distance of 0.15D from same point at downstream. In radial direction domain was considered up to a distance of 0.15D from the axis of the hub. This peripheral plane is called far-field boundary.

The propeller computational domain is cylindrical shape surrounding the propeller where a rotational cylinder with sufficient larger diameter than the propeller diameter enfolds the propeller in its cross section center and allows the fluid to pass by the model. The rotating zone was solved via Frame Motion. ANSYS is used to mesh the entire domain of propeller. Domain is discretized using Triangular elements. Convergence is checked with element sizes 10 and 12.Close results are observed for element size 10 and 12.
Element size 10 is used for mesh generation. After discretization number of elements in the domain are 7363445.

3.2 Boundary Conditions

In the present case propeller is used in warships consist of five blades. The diameter of propeller is 0.4m and hub to propeller diameter is 0.389. In the present simulations for prediction of non-cavitation noise of propeller is carried out at rotating speeds of propeller at 780rpm & 840rpm and the speed of war ship is 6.66m/s & 7.17m/s. The noise produced by a propeller is very much importance to warship designers and military strategists for many years. So in this case an attempt is made to prediction of non-cavitation noise of propeller using of FW-H equation coupled with DES computer code based on cell-centered finite volume method (FVM) on unstructured meshes for viscous flow field around propeller. The time step size is given as 0.000254s.The iterative time steps is given as 600. Solution allowed to converge when changes in solution variables from one iteration to the next is negligible i.e., 0.001. In the following table the boundary conditions are shown.

Table 1: shows the boundary conditions.

Pressure Link	SIMPLE
Pressure	Standard
Discretization scheme	Second Order Upwind

Turbulence model	Detached Eddy Simulation
Sub-Grid Scale Model	Smagorinsky-Lilly
Mesh type	Unstructured Triangular Mesh
Motion type	Frame motion
Near Wall Treatment	Standard wall functions
Acoustic Models	Ffowcs Williams - Hawking's
Solver	Unsteady

The dimensions of the propeller Aluminium alloy2345 are mentioned as below

Table 2: Principle particulars of propeller model

Diameter of the Propeller	0.4m
EAR= A_E/A_0	0.58
No. of Blades	5
Hub ratio	0.389
Series	Naca

Table 3: Different parameters of flow and acoustic conditions.

Sl. No	Va (m/s)	N (rpm)	Turbulence model	ρ(kg/m3)	a_0 (m/s)	P_{ref} (Pa)
1	6.66	780	DES	1020	1500	10^{-6}
2	7.17	840	DES	1020	1500	10^{-6}

In table (3), N is rotational speed, Va is axial velocity of flow, ρ is density of water, a0 is sound velocity and P_{ref} is reference pressure in underwater. In this Numerical simulation four Hydrophones is used for extraction Sound Pressure Levels (SPLs).

The Position of Hydrophones and their coordinates are shown in Figure 2 and Table 4.

Table 4: Coordinates of different Hydrophones

Name	X-Cord.(m)	Y-Cord.(m)	Z-Cord.(m)
Hydrophone 1	1	0	0
Hydrophone 2	0	0	-1
Hydrophone 3	0	1	0
Hydrophone 4	-1	0	0

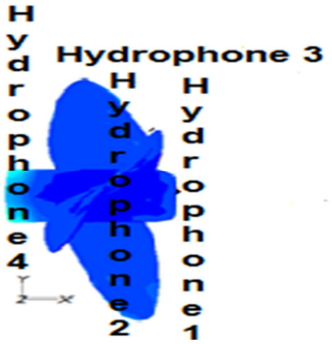

Figure 2: Positions of Hydrophones

4.0 RESULT AND DISCUSSION

In this study we were studied non-cavitating noise in order to find the ranges of the Sound Pressure Levels, its development and to study the effect of non-cavitation noise on the SPL's. These results are compared with experiments conducted in cavitation tunnel of size 1x1x6m. Since hydrophone 1 is located near sound source, the overall SPL for hydrophone 1 is less than hydrophone 4. As can be seen from results ranges of SPL's increase with increasing rotational speed of propeller.

The non-cavitating noise generated by an underwater propeller is analyzed numerically in this study. The flow field is analyzed with finite volume method (FVM), and then CFD data are used as the input for Ffowcs Williams–Hawkings formulation to predict the far-field acoustics. Noise characteristics are presented according to noise sources and conditions. According to results non-cavitation noise going to incept by increase of flow velocity and propeller revolution speed.

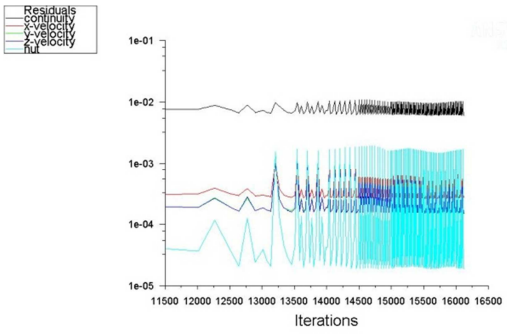

Figure 3: Convergence graph

The graph represents the convergence history of the propeller sound pressure levels. The convergence criteria are considered as the difference between the values of the succeeding and preceding are in the range of 0.001.

4.1 Pressure and Velocity Contours

The figures 4 & 5 represent the Contours of the Pressure and Velocities at various sections of the propeller.

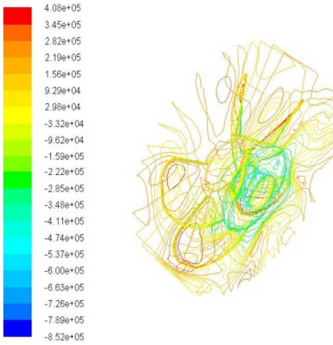

Figure 4: Contours of Static Pressures (Pa) representing inlet, outlet, outer, wall solid.

Figure 5: Contours of Velocity (m/s) of inlet, outlet, and wall solid.

The pressure and velocity contours for operating condition 2 are shown in below figures 6 and 7.

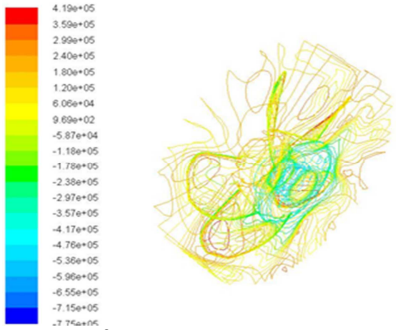

Figure 6: Contours of Static Pressures (Pa) representing inlet, outlet, outer, wall solid.

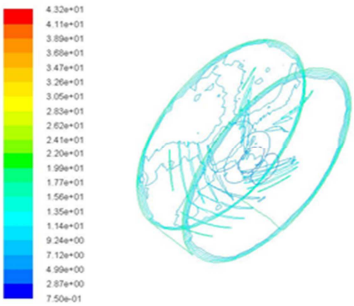

Figure 7: Contours of Velocity (m/s) of inlet, outlet, and wall solid.

4.2 Acoustic Graphs:

The following figures 8, 9, 10, 11 represents the Sound Pressure Levels of propeller for various Hydrophones placed at various positions for different operating conditions.

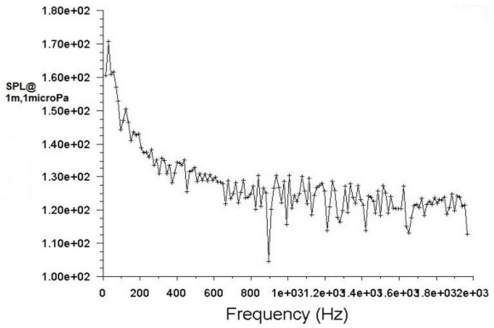

Figure 8: Noise prediction graph up to 2000 Hz for receiver1 positioned at 1m along x-direction for operating condition one.

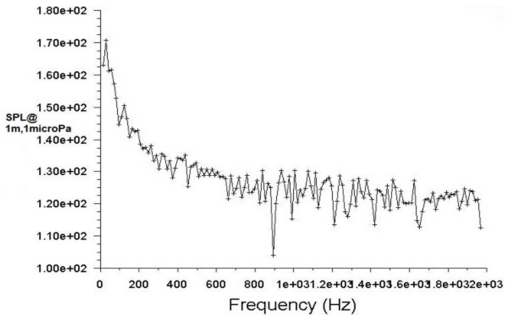

Figure 9: Noise prediction graph up to 2000 Hz for receiver2 positioned at 1m along transverse –z direction for operating condition.

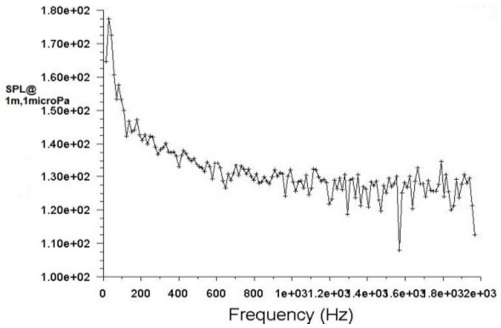

Figure 10: Noise prediction graph up to 2000 Hz for receiver1 positioned at 1m along x-direction for operating condition 2.

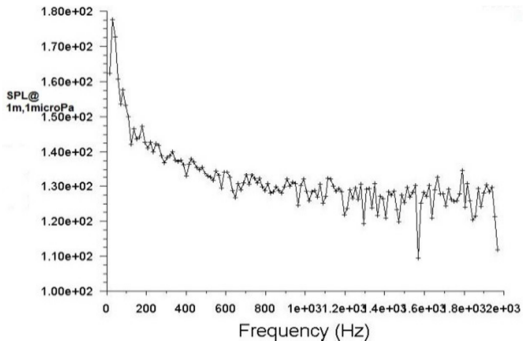

Figure 11: Noise prediction graph up to 2000 Hz for receiver2 positioned at 1m along transverse y-direction operating condition 2.

5.0 CONCLUSION

The propeller is assumed to be operated at 780 rpm & 840rpm with forward velocity of 6.66m/s & 7.17m/s for all noise predictions. From the two operating conditions we noticed that propeller operating at 6.66m/s and 780 rpm yields lower noise than at other operating condition it 152dB. Noise prediction graph clearly shows that peak SPL values are observed at first BPF and at the second order harmonic and these are predominated at low frequency only. The basic noise source in propeller is dipolar noise source as generated due to hydrodynamic pressure fluctuation

ACKNOWLEDGEMENTS

The authors wish to express their sincere gratitude to Sri V. Rama Krishna, Scientist'D', NSTL, Visakhapatnam and Mrs. C. Neelima Devi, Assistant Prof., University College of Engineering, Vizianagaram,JNTUK.

REFERENCE

1. Münir Cansın Özden1, Ahmet Gültekin Avcı1 and Emin Korkut1 *A Numerical Study on Prediction of Noise Characteristics Generated By a Propeller*, Istanbul Technical University, Faculty of Naval Architecture and Ocean Engineering, Maslak-Istanbul, Turkey34469.
2. Bagheri M.R, Seif M.S, and Mehdigholi H, *Numerical Simulation of Underwater Propeller Noise*, Journal of Ocean, Mechanical and Aerospace -Science and Engineering-, Vol.4.
3. Morgut, M., Nobile, E. *"Influence of grid type and turbulence model on the numerical prediction of the flow around marine propellers working in uniform inflow."* Ocean Eng., Vol. 42, pp. 26-34, 2012.
4. Hand book of Acoustics by Malcolin J.Crocker, *in different types of noises and their effects and the propeller characteristics* were explained.
5. The *effects of noises in the marine propellers and their effects and remedies* are explained in the book of Marine Propellers and Propulsions by John Carlton.
6. International conference on Vibration and Acoustic, Iran, Sharif University of Technology.
7. Light hill, *on sound generated aerodynamically*. I. General theory, Pros, R. Soc. Lond, vol. MJ. (1952). 211 no. 1107 564-587.
8. Spalart, P.R. *"Detached-Eddy Simulation," Ann.* Rev. Fluid Mech., Vol. 41, pp. 181-202, 2009.
9. Sebastien D., *"Recent Improvements in the Zonal Detached Eddy Simulation (ZDES) formulation*, "Theory. Comp. Fluid Dyn. Vol. 26, pp.1-28, 2011.
10. Rui Z., Chao Y., Li X., Kong, W. *"Towards an Entropy-based Detached-Eddy Simulation,"* Science China Physics, Mechanics and Astronomy, Vol. 56, No. 10, pp. 1970-1980, 2013.